AFWAL-TR-81-3087

AD A108836

A FINITE ELEMENT METHOD FOR COMPUTING SOUND PROPAGATION IN DUCTS CONTAINING FLOW

Dennis W. Quinn
Analysis and Optimization Branch
Structures and Dynamics Division

September 1981

Final Report for the Period December 1975 to May 1981

Approved for public release; distribution unlimited.

FLIGHT DYNAMICS LABORATORY
AIR FORCE WRIGHT AERONAUTICAL LABORATORIES
AIR FORCE SYSTEMS COMMAND
WRIGHT-PATTERSON AIR FORCE BASE, OHIO 45433

NOTICE

When Government drawings, specifications, or other data are used for any purpose other than in connection with a definitely related Government procurement operation, the United States Government thereby incurs no responsibility nor any obligation whatsoever; and the fact that the government may have formulated, furnished, or in any way supplied the said drawings, specifications, or other data, is not to be regarded by implication or otherwise as in any manner licensing the holder or any other person or corporation, or conveying any rights or permission to manufacture, use, or sell any patented invention that may in any way be related thereto.

This report has been reviewed by the Information Office (OI) and is releasable to the National Technical Information Service (NTIS). At NTIS, it will be available to the general public, including foreign nations.

This technical report has been reviewed and is approved for publication.

Paul J. Nikolai
PAUL J. NIKOLAI
Task Scientist

Fred A. Picchioni
FREDERICK A. PICCHIONI, LtCol, USAF
Chief, Analysis & Optimization Branch

FOR THE COMMANDER

Ralph L. Kuster
RALPH L. KUSTER, Colonel, USAF
Chief, Structures & Dynamics Division

"If your address has changed, if you wish to be removed from our mailing list, or if the addressee is no longer employed by your organization please notify AFWAL/FIBR *,W-PAFB, OH 45433 to help us maintain a current mailing list".*

Copies of this report should not be returned unless return is required by security considerations, contractual obligations, or notice on a specific document.

Unclassified

SECURITY CLASSIFICATION OF THIS PAGE *(When Data Entered)*

REPORT DOCUMENTATION PAGE	READ INSTRUCTIONS BEFORE COMPLETING FORM
1. REPORT NUMBER: AFWAL-TR-81-3087	2. GOVT ACCESSION NO.: AD-A108 836
	3. RECIPIENT'S CATALOG NUMBER
4. TITLE *(and Subtitle)*: A FINITE ELEMENT METHOD FOR COMPUTING SOUND PROPAGATION IN DUCTS CONTAINING FLOW	5. TYPE OF REPORT & PERIOD COVERED: Technical - Final Dec 75 - May 81
	6. PERFORMING ORG. REPORT NUMBER
7. AUTHOR(s): Dennis W. Quinn	8. CONTRACT OR GRANT NUMBER(s)
9. PERFORMING ORGANIZATION NAME AND ADDRESS: Flight Dynamics Laboratory (AFWAL/FIBR) Air Force Wright Aeronautical Laboratories Wright-Patterson AFB, Ohio 45433	10. PROGRAM ELEMENT, PROJECT, TASK AREA & WORK UNIT NUMBERS: 61102F 2304N112
11. CONTROLLING OFFICE NAME AND ADDRESS: Flight Dynamics Laboratory (AFWAL/FIB) Air Force Wright Aeronautical Laboratories Wright-Patterson AFB, Ohio 45433	12. REPORT DATE: September 1981
	13. NUMBER OF PAGES: 31
14. MONITORING AGENCY NAME & ADDRESS *(if different from Controlling Office)*	15. SECURITY CLASS. *(of this report)*: Unclassified
	15a. DECLASSIFICATION/DOWNGRADING SCHEDULE

16. DISTRIBUTION STATEMENT *(of this Report)*

Approved for public release; distribution unlimited.

17. DISTRIBUTION STATEMENT *(of the abstract entered in Block 20, if different from Report)*

18. SUPPLEMENTARY NOTES

19. KEY WORDS *(Continue on reverse side if necessary and identify by block number)*

Duct Acoustics
Finite Elements
Finite Differences
Conformal Mapping
Wave Equation
Helmholtz Equation
Jet Noise

20. ABSTRACT *(Continue on reverse side if necessary and identify by block number)*

In this report, solutions of the equations which describe sound propagation in nonuniform ducts containing flow are computed with a finite element approach. A least squares approach is considered and compared to a Galerkin approach. The least squares problem is solved using an iterative method and compared with results obtained using direct Gaussian elimination. The accuracy of linear basis functions on triangles, bilinear basis functions on rectangles, and biquadratic basis functions on rectangles are compared. For the nonuniform ducts, the use of quadrilaterals as elements and an isoparametric map are

DD FORM 1 JAN 73 1473 EDITION OF 1 NOV 65 IS OBSOLETE

Unclassified

SECURITY CLASSIFICATION OF THIS PAGE *(When Data Entered)*

considered. The biquadratics permit good approximation of curved boundaries and better convergence than the bilinear basis functions. Consequently, the finite element solution space consists of piecewise biquadratics defined on the finite element discretization of the geometry of the duct. Acoustic fields within uniform ducts both with and without flow have been computed and compare well with modal solutions and finite difference solutions. For nonuniform ducts without flow, the computed acoustic fields also compare well with exact or other computed solutions. For the case of two-dimensional flow within nonuniform ducts, sample calculations favorably compare with other solutions or limiting cases.

FOREWORD

This report describes work performed in the Structures and Dynamics Division, Flight Dynamics Laboratory, Air Force Wright Aeronautical Laboratories and in the College of Engineering, Air Force Institute of Technology, under the Defense Research Sciences Program, Project 2304, Mathematical and Information Sciences, Task N1, Computational Aspects of Fluid and Structural Mechanics. It constitutes the Final Report of Work Unit 2304N112, Duct Acoustics Research, describing work accomplished between December 1975 and May 1981.

The author expresses his appreciation to Ms. Jean Schwab for running the computer programs, to Dr. Jon Lee for discussions concerning fluid flows and to Dr. Karl G. Guderley for pointing out to the author the additional source of error in the least squares approach.

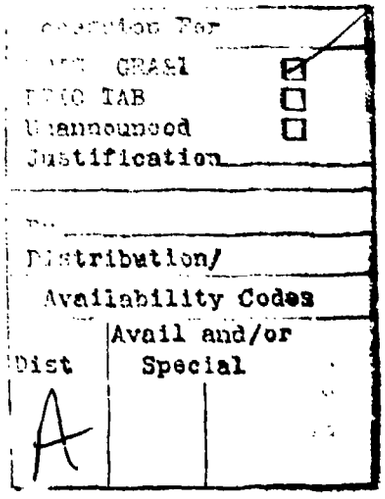

TABLE OF CONTENTS

LIST OF ILLUSTRATIONS

SECTION I

INTRODUCTION

Duct acoustics continues to be of great interest to the aircraft industry because of the need of obtaining quieter aircraft by inserting sound absorbing linings in jet engines. When considering a reasonably detailed representation of an aircraft engine, one obtains a system of linear differential equations with nonconstant coefficients to be solved in a region with a complicated nonuniform geometry. Earlier, we used a finite difference method with a conformal map to determine sound pressure levels within nonuniform ducts in the absence of flow (References 1 and 2). However, for all but a few duct geometries the conformal map must be determined numerically, and this can be a complicated problem in itself. An integral equation method was used in Reference 3 to solve the no-flow equations in both uniform and nonuniform ducts. This method is very efficient in terms of computational time and does not require a mapping to a uniform geometry. However, for the problem of flow in a nonuniform duct, the acoustic equations have variable coefficients. The fundamental solution, which is needed in the integral equation method, is not known. With the finite element method, we are able to handle complicated nonuniform geometries and also take advantage of the high order convergence of the higher order finite element methods. For these reasons, we have decided to evaluate the finite element method for solving problems in duct acoustics. Because of the great versatility of the finite element method, there are many alternatives to consider. For instance, a least squares approach could be used, and the resulting positive definite system of equations (called the stiffness matrix by the structural engineers) could be solved by an iterative method. The use of an iterative method had been considered and rejected for finite differences because the finite difference system of equations was not positive definite and, hence, not compatible with an iterative solution technique. However, the system of equations which arises from a least squares finite element approach is positive definite and can be solved iteratively.

A problem with the least squares approach is that it introduces an additional source of error which does not occur with a Galerkin finite element approach. So perhaps a Galerkin approach should be used. This can be viewed as a type of weak solution of the differential equations in question or as a method of weighted residuals. The system of equations which results when a Galerkin approach is used to solve the Helmholtz equation is not positive definite and, therefore, cannot be solved iteratively. If a direct solver is used, the decision has to be made whether to make it in-core or out-of-core on the computer at hand.

Once the basic approach has been decided, a choice of basis or shape functions must be made. The two choices considered in this paper are piecewise linear and piecewise quadratic polynomials. The accuracy of these two different systems of basis functions are compared as well as their respective computational times. Related to the choice of basis function is the way that the duct geometry is divided into elements. One possibility considered was the use of rectangles and triangles with the triangles used to improve the approximation of the boundary of a non-uniform duct. A second approach consists of using only quadrilaterals with perhaps curved sides to approximate the boundary. Results were consistent with others (Reference 4) in the discovery that, in general, triangles have lower accuracy than rectangles or quadrilaterals for many classes of problems. Since the polynomials and products of polynomials which comprise the basis functions need to be integrated, it has to be decided whether to integrate exactly or to use numerical quadrature. These questions and alternatives have been addressed and will be discussed in subsequent sections of this paper.

One of the most difficult decisions to be made when solving duct acoustics problems in nonuniform ducts is choosing the type of flow. The flow considered is that which corresponds to uniform mean flow in a uniform duct. This flow field then provides the coefficients in the acoustic equations.

As the results indicate, the finite element method offers simplicity of use once the initial programming and bookkeeping efforts are completed and is accurate when compared to competing methods such as finite differences. The advantage that nonuniform geometries are more easily handled by finite elements versus finite differences is not as great when the mapping function is used to compute the flow field. This is because the same mapping function could be used to map the nonuniform duct to a rectangular duct with the acoustic equations on the rectangle then solved by finite differences.

In Section II the derivation of the acoustic equations and boundary conditions will be described, in Section III the finite element solution method will be discussed and in Section IV the results will be presented. For other references using the finite element method to solve duct acoustics problems, see References 5-8.

SECTION II

DERIVATION OF THE EQUATIONS

1. DIFFERENTIAL EQUATIONS

If viscous and heat transfer terms are neglected, the equations of motion for an ideal gas are:

Momentum	$\rho' \, D(\vec{V}')/Dt = -\nabla p'$	(a)	
Continuity	$D(\rho')/Dt + \rho'(\nabla \cdot \vec{V}') = 0$	(b)	(1)
Energy and state	$p' = \text{const} \, \rho^{\alpha}$	(c)	

where ρ' is the density, $\vec{V}'$ is the velocity vector, and p' is the pressure.

Equations 1 can be combined to form the usual conservation of mass and momentum equations:

$$\frac{\partial \rho'}{\partial t} + \vec{V}' \cdot \nabla p' + \rho' \nabla \cdot \vec{V}' = 0$$

$$\rho' \left(\frac{\partial \vec{V}'}{\partial t} + \vec{V}' \cdot \nabla \vec{V}' \right) = -\nabla p' \qquad (2)$$

Because of the application to aircraft engines, these equations have been written in cylindrical coordinates and become:

$$\frac{\partial \rho'}{\partial t} + u' \frac{\partial \rho'}{\partial z} + v' \frac{\partial \rho'}{\partial r} + \frac{w'}{r} \frac{\partial \rho'}{\partial \theta}$$

$$+ \rho' \left[\frac{\partial u'}{\partial z} + \frac{\partial v'}{\partial r} + \frac{1}{r} \frac{\partial w'}{\partial \theta} + \frac{v'}{r} \right] = 0$$

$$\rho' \left[\frac{\partial u'}{\partial t} + u' \frac{\partial u'}{\partial z} + v' \frac{\partial u'}{\partial r} + \frac{w'}{r} \frac{\partial u'}{\partial \theta} \right] = \frac{-\partial p'}{\partial z}$$

$$\rho' \left[\frac{\partial v'}{\partial t} + u' \frac{\partial v'}{\partial z} + v' \frac{\partial v'}{\partial r} + \frac{w'}{r} \frac{\partial v'}{\partial \theta} - \frac{w'^2}{r} \right] = \frac{-\partial p'}{\partial r}$$

$$\rho' \left[\frac{\partial w'}{\partial t} + u' \frac{\partial w'}{\partial z} + v' \frac{\partial w'}{\partial r} + \frac{w'}{r} \frac{\partial w'}{\partial \theta} + \frac{1}{r} v' w' \right]$$

$$= \frac{-\partial p'}{\partial \theta} \frac{1}{r} \qquad (3)$$

If u', v', w', p', and ρ' are each written as the sum of a mean quantity and a small fluctuating acoustic quantity, ie., $u' = \bar{u} + u$, $v' = \bar{v} + v$,

$w' = \bar{w} + w$, $p' = \bar{p} + p$, and $\rho' = \bar{\rho} + \rho$, where the mean quantities are independent of time and satisfy the steady mean flow equations and where products of the fluctuating quantities are considered negligible, then Equations 3 become:

$$i\omega p + \bar{u}\frac{\partial p}{\partial z} + \bar{v}\frac{\partial p}{\partial r} + \frac{\bar{w}}{r}\cdot mp$$

$$+ \gamma p\left[\frac{\partial \bar{u}}{\partial z} + \frac{\partial \bar{v}}{\partial r} + \frac{1}{r}\frac{\partial \bar{w}}{\partial \theta} + \frac{\bar{v}}{r}\right] + \frac{\partial \bar{p}}{\partial z}\,u + \frac{\partial \bar{p}}{\partial r}\cdot v$$

$$+ \frac{\partial \bar{p}}{\partial \theta}\cdot\frac{w}{r} + \gamma\bar{p}\left(\frac{\partial u}{\partial z} + \frac{\partial v}{\partial r} + \frac{v}{r} + \frac{m}{r}w\right) = 0 \qquad (a)$$

$$\left(i\omega + \frac{\partial \bar{u}}{\partial z} + \frac{\bar{w}}{r}m\right)u + \bar{u}\frac{\partial u}{\partial z} + \bar{v}\frac{\partial u}{\partial r} + \frac{\partial \bar{u}}{\partial r}v$$

$$+ \frac{1}{r}\frac{\partial \bar{u}}{\partial \theta}w + \frac{1}{\rho\bar{c}^2}\left(\bar{v}\frac{\partial \bar{u}}{\partial r} + \frac{\bar{w}}{r}\frac{\partial \bar{u}}{\partial \theta} + \bar{u}\frac{\partial \bar{u}}{\partial z}\right)p$$

$$+ \frac{1}{\bar{\rho}}\frac{\partial p}{\partial z} = 0 \qquad (b)$$

$$\left(i\omega + \frac{\partial \bar{v}}{\partial r} + \frac{\bar{w}}{r}m\right)v + \bar{u}\frac{\partial v}{\partial z} + \bar{v}\frac{\partial v}{\partial r} + \frac{\partial \bar{v}}{\partial z}u \qquad (4)$$

$$+ \left(\frac{1}{r}\frac{\partial \bar{v}}{\partial \theta} - \frac{2\bar{w}}{r}\right)w + \frac{1}{\rho\bar{c}^2}\left(\bar{u}\frac{\partial \bar{v}}{\partial z} + \bar{v}\frac{\partial \bar{v}}{\partial r} + \frac{\bar{w}}{r}\frac{\partial \bar{v}}{\partial \theta}\right)p$$

$$+ \frac{1}{\bar{\rho}}\frac{\partial p}{\partial r} = 0 \qquad (c)$$

$$\left(i\omega + \frac{\bar{w}}{r}m + \frac{1}{r}\frac{\partial \bar{w}}{\partial \theta} + \frac{\bar{v}}{r}\right)w + \bar{u}\frac{\partial w}{\partial z} + \bar{v}\frac{\partial w}{\partial r}$$

$$+ \frac{\partial \bar{w}}{\partial z}u + \left(\frac{\partial \bar{w}}{\partial r} + \frac{\bar{w}}{\bar{\rho}r}\right)v + \frac{1}{\bar{\rho}\bar{c}^2}\left(\bar{u}\frac{\partial \bar{w}}{\partial z} + \bar{v}\frac{\partial \bar{w}}{\partial r}\right.$$

$$\left. + \frac{\bar{w}}{r}\frac{\partial \bar{w}}{\partial \theta}\right)p + \frac{1}{\bar{\rho}}\frac{m}{r}p = 0 \qquad (d)$$

In Equations 4, time dependence is assumed to be of the form $e^{i\omega t}$ while θ dependence is assumed to be of the form $e^{im\theta}$. In addition, the equation $p = c^2\rho$ has been used to eliminate ρ from the equations. Therefore, the equations contain only derivatives with respect to z, the axial coordinate, and r, the radial coordinate, and the duct can be taken to be two-dimensional. Equations 4 will be used in Section III in the finite element formulation of the duct acoustics problems to be considered.

2. BOUNDARY CONDITIONS

Because of the form of the differential Equations 4, the appropriate boundary conditions are the specification of either the pressures, the velocities or setting the ratio of the pressure and velocity equal to a given impedance around the boundary of the duct. Because of the assumption of axial symmetry along the part of the boundary corresponding to r = 0, the radial component of the velocity is set to zero. Along the entrance of the duct the pressure distribution is specified while at the exit area of the duct the ratio of the exit velocity and pressure are set equal to the exit impedance. These conditions can be specified independently of the flow within the duct. However, at the outer wall where sound absorbing liner is located, the general form of the boundary condition depends on the flow if slip is permitted. That is, at the outer wall the boundary condition is

$$u\, n_x + v\, n_r = p/z - i\frac{u_o\, n_x + v_o\, n_r}{\omega}\frac{\partial}{\partial \tau}(p/z) \qquad (5)$$

where $\hat{n} = (n_x, n_r)$ is the unit outer normal to the boundary at the point (x,r). Note that in the case of no-slip on the boundary, $u_o\, n_z + v_o\, n_r = 0$, so that Equation 5 reduces to $u\, n_x + v\, n_r = p/z$.

SECTION III

THE FINITE ELEMENT METHOD

1. LEAST SQUARES METHOD

Because of the attractiveness of solving large systems of equations by using an iterative method, the first attempt at solving acoustic problems with a finite element method was with a least squares method. For iterative methods to converge, it is necessary that the system to be solved be positive definite (Reference 9). However, if a straight-forward finite element approach is taken with the acoustic equations, the resulting system will not be positive definite. On the other hand, the system of equations resulting from a least squares approach will be positive definite and, therefore, amenable to an iterative method. The least squares formulation of the problem consisted of squaring the left-hand side of Equations 4a-d, summing the squares, integrating the sum of squares over the area of the duct, and then minimizing this expression as a functional of the variables p, u, v, w. In this formulation the boundary conditions were imposed by writing them as an equation with vanishing right-hand side, squaring this equation, integrating it over the boundary and adding this line integral to the area integral already obtained.

The functions p, u, v, w were written as linear combinations of piecewise polynomial functions defined over rectangular and triangular subdivisions of the duct, and these linear combinations were substituted into the aforementioned functional. In this way, the functional was then a function of 4 N unknown variables instead of a functional. There were 4 N variables because each of four functions p, u, v, w was written as a combination of N piecewise polynomials so there were N unknown coefficients for each function or a total of 4 N unknowns to determine. The usual procedure of differentiating this function with respect to each of the variables and setting each equal to zero results in 4 N equations to be solved.

Although the solutions obtained from the least squares approach were qualitatively correct and quantitatively adequate, when compared to finite difference solutions requiring approximately the same computational effort

they were not nearly as accurate. The following example illustrates the source of error in the least squares approach which caused the poor comparison with finite differences when both were compared to an exact solution. Suppose the ordinary differential equation and boundary conditions to be solved are

$$y'' + y = 0,\ y(0) = 0,\ y(1) = 1 \qquad (6)$$

on the interval between zero and one. A typical least squares formulation would be to minimize the functional

$$J(y) = \int_0^1 (y'' + y)^2\, dx \qquad (7)$$

over the solution space of all functions having an integrable second derivative which vanish at $x = 0$ and equal one at $x = 1$. However, if the first variation of this functional is taken, the Euler equation obtained is

$$y^{IV} + 2\, y'' + y = 0 \qquad (8)$$

with the additional natural boundary conditions

$$(y'' + y) = 0 \text{ at } x=0 \text{ and } (y'' + y) = 0 \text{ at } x=1 \qquad (9)$$

Now the general solution of the differential Equation 6 is $y = a \sin(x) + b \cos(x)$ and the boundary conditions require that $b = 0$ and $a = 1/\sin(1)$. Therefore, the solution to Equation 6 is $y = \sin(x)/\sin(1)$. The general solution of differential Equation 8 is $y = a \sin(x) + b \cos(x) + c\, x \sin(x) + d\, x \cos(x)$. If the boundary conditions, Equation 9 are satisfied exactly, then $c = 0$ and $d = 0$, and the requirement that the solution vanishes at $x = 0$ and equals one at $x = 1$ yields $y = \sin(x)/\sin(1)$. Therefore, if the natural boundary conditions are satisfied exactly, the functional Equation 8 yields the correct solution. But if Equation 7 is minimized approximately using the finite element method, then Equation 9 will not be satisfied exactly, and consequently the coefficients c and d will not vanish. Hence, the finite element solution will contain contributions from the two spurious functions $y_3 = x \sin(x)$ and $y_4 = x \cos(x)$. This is the additional error that one encounters when using a least squares finite element method which is basic to the problem and not caused by

nonconforming elements. As a result of this additional error, a finer discretization is required than would be necessary if it were not present. If the iterative solution of the least squares problem were sufficiently quicker in terms of computer time to offset the additional computational work required as a result of the finer mesh, then the least squares method would still be preferable to a Galerkin method which requires a direct system solver. To compare the two possibilities, the equations were solved using both the iterative approach and direct Gaussian elimination and the computational times were compared. For a system with 314 unknowns and a bandwidth of 42 (42 non-zero entries in any given row and all of these entries clustered about the main diagonal), a moderately accurate iterative solution was obtained with 41 iterations taking 14 seconds of CP time and 373 seconds of input-output time on the computer. For the same problem, the direct Gaussian elimination took only 3 seconds of CP time and 10 seconds of input/output time. The conclusion was, therefore, that for the size matrices considered, a direct solver was preferred to an iterative method. Because the major attraction of the least squares method was the possibility of solving the large system of equations iteratively and since the iterative methods did not turn out to be less expensive computationally, it was decided to use a Galerkin or weak solution method. The integral or weak form of the equations will now be described.

2. THE INTEGRAL FORM OF THE EQUATIONS

To avoid rewriting Equations 4 repeatedly, it will be represented by:

$$\begin{aligned} D1(p,u,v,w) &= 0 \quad (a) \\ D2(p,u,v,w) &= 0 \quad (b) \\ D3(p,u,v,w) &= 0 \quad (c) \\ D4(p,u,v,w) &= 0 \quad (d) \end{aligned} \qquad (4)$$

Then the weak or integral form of Equations 4 is obtained by multiplying each of the equations by the product of the variable r and a test function (weight function) and integrating over the area of the duct. In this way the requirement that the solutions of Equations 4 have continuous first

derivatives within the duct is relaxed to the requirement that they have generalized first derivatives which are integrable. The integral form of Equations 4 is written as

$$\begin{aligned} &\iint r\, f\, D1(p,u,v,w)\, dz\, dr = 0 \qquad (a)\\ &\iint r\, f\, D2(p,u,v,w)\, dz\, dr = 0 \qquad (b)\\ &\iint r\, f\, D3(p,u,v,w)\, dz\, dr = 0 \qquad (c)\\ &\iint r\, f\, D4(p,u,v,w)\, dz\, dr = 0 \qquad (d) \end{aligned} \qquad (10)$$

where f is a test function. The boundary conditions relating the ratio of the pressure and velocity to the impedance are specified by integrating some of the terms in Equation 10a by parts.

The particular integration by parts is

$$\begin{aligned} &\iint \gamma f\, p_o \left(r \frac{\partial u}{\partial z} + r \frac{\partial v}{\partial r} + v + m\, w\right) dz\, dr\\ &= \int \gamma r\, f\, p_o\, (u\, n_z + v\, n_r)\, ds + \iint \Big[\gamma f\, p_o\, m\, w \qquad (11)\\ &- \gamma r \left(\frac{\partial p_o}{\partial z} f + p_o \frac{\partial f}{\partial z}\right) u - \gamma r \left(\frac{\partial p_o}{\partial r} f + p_o \frac{\partial f}{\partial r}\right) v \Big]\, dz\, dr \end{aligned}$$

Therefore, the term in Equation 10a which corresponds to the left-hand side of Equation 11 is replaced by the right-hand side of Equation 11. This new version of Equation 10a will be denoted as Equation 10a'.

A finite element solution of Equations 10a', b, c, and d consists of first dividing the interior of the duct into a collection of rectangles and triangles and then distributing an appropriate number of grid points or nodes on the sides and in the interior of these triangles and rectangles. Figure 1 indicates a typical finite element discretization of two difference duct shapes. If piecewise linear basis functions (shape functions) are to be used on triangles then a node at each of the vertices of each of the triangles is appropriate. If piecewise linear basis functions are to be used on rectangles then a node at each of the vertices of each rectangle is appropriate. A node at each vertex, a node at the midpoint of each side and a node at the center of each rectangle for a total of nine nodes is appropriate if piecewise biquadratic basis functions

are to be used. In Figure 2, the location of nodes on triangles and rectangles is indicated. Whatever the choice of basis function, the next step is to write p,u,v,w each as a linear combination of the basis functions. That is,

$$p(z,r) = \sum_{j=1}^{N} p_j \, g_j(z,r)$$

$$u(z,r) = \sum_{j=1}^{N} u_j \, g_j(z,r)$$

$$v(z,r) = \sum_{j=1}^{N} v_j \, g_j(z,r)$$

$$w(z,r) = \sum_{j=1}^{N} w_j \, g_j(z,r) \qquad (12)$$

where each g_j is a basis function, the p_j, u_j, v_j and w_j are unknown coefficients to be determined, and N is the number of basis functions.

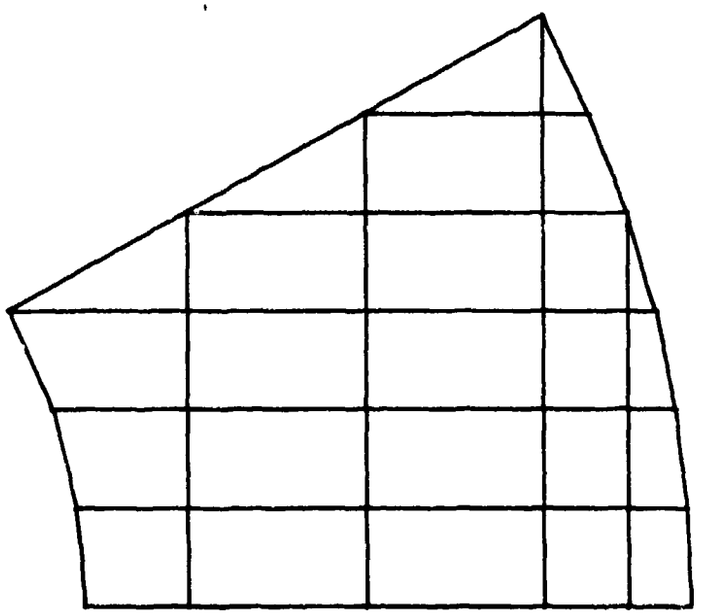

Figure 1a. Discretization of a Conical Duct

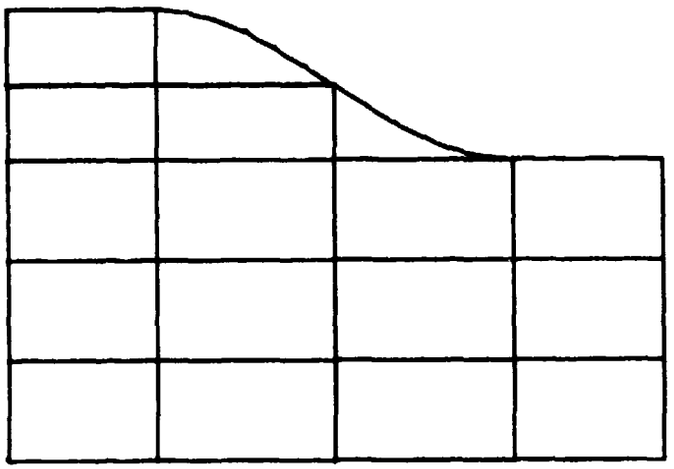

Figure 1b. Discretization of a Tapered Duct

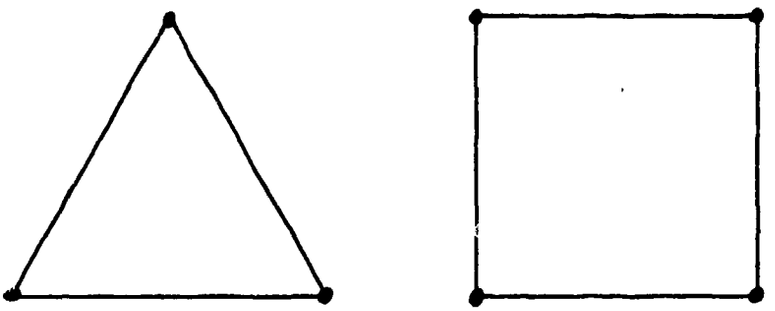

Linear Elements

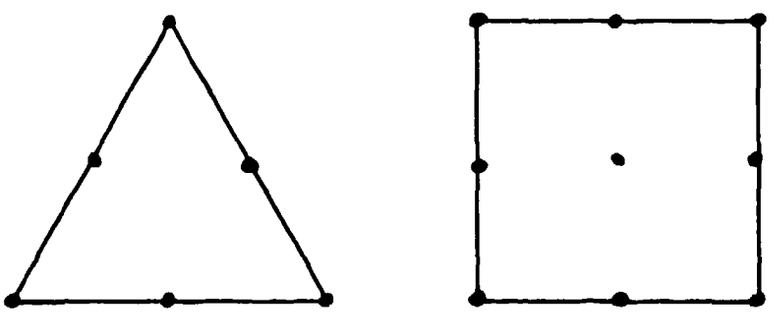

Quadratic Elements

Figure 2. Distribution of Nodes on Linear and Quadratic Elements

The g_j are determined by requiring the jth function to be 1 at the jth node and to vanish at all other nodes. Typically this is done on an element basis; that is, the nine biquadratic basis functions which are nonzero within a rectangle are determined by specifying each to be one at one node on the rectangle and vanish at the other eight nodes. In this way a system of equations is obtained which determines the coefficients of the nine biquadratic basis functions. Once the g_j have been determined, the expression for p,u,v,w defined by Equations 12 are substituted into Equations 10a', b, c, and d. The test function f which appears in Equations 10 is set equal to each of the functions g_j for j = 1 through j = N. In this way 4 N algebraic equations are obtained which determine the 4 N unknown coefficients $p_1, \ldots, p_N, u_1, \ldots, u_N, v_1, \ldots, v_N, w_1, \ldots, w_N$. Then if the value of p,u,v or w is needed anywhere within the duct, Equation 12 is used with the computed values of the coefficients in Equation 12.

Because of the large system of equations which arises in the determination of the p_j's, u_j's, v_j's, and w_j's, an out-of-core solver is almost mandatory. Even for a relatively coarse discretization of 5 x 5 elements with biquadratic basis functions, there are 121 nodes and consequently 484 equations to be solved. Even with a system solver which accounts for a bandwidth of only 200, to keep the entire banded system, right-hand side and auxiliary vectors in core requires 96,800 memory locations. This is almost 300,000 octal locations, the maximum core available with the CDC CYBER machines at the ASD Computer Center at Wright-Patterson. Therefore, an out-of-core banded solver is used which requires a moderate amount of in-core storage but much more input/output time.

Because of the ease of switching from linear to quadratic basis functions (Figure 3 shows the ease in changing from one mesh to the other), it was decided to compare the accuracy of the two types of basis functions in deciding which to use. The following problem was solved on the same grid on a rectangular duct. The differential equation was the Helmholtz equation written in system form,

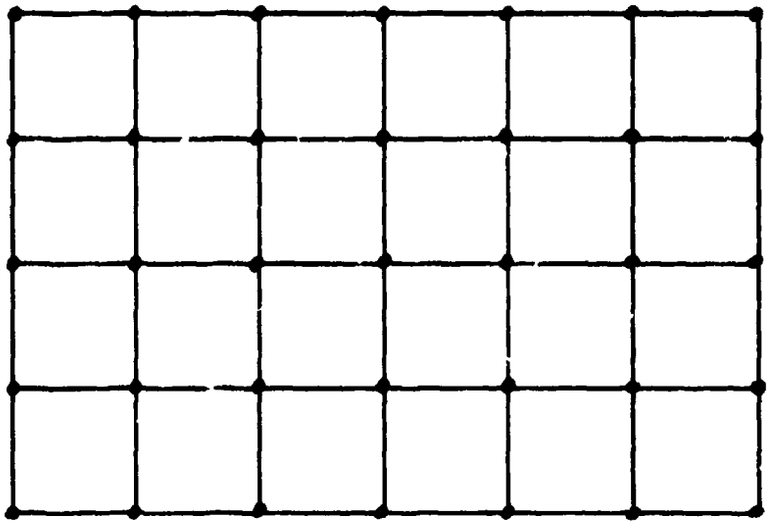

Figure 3a. Location of 35 Nodes on Rectangle with Linear Elements

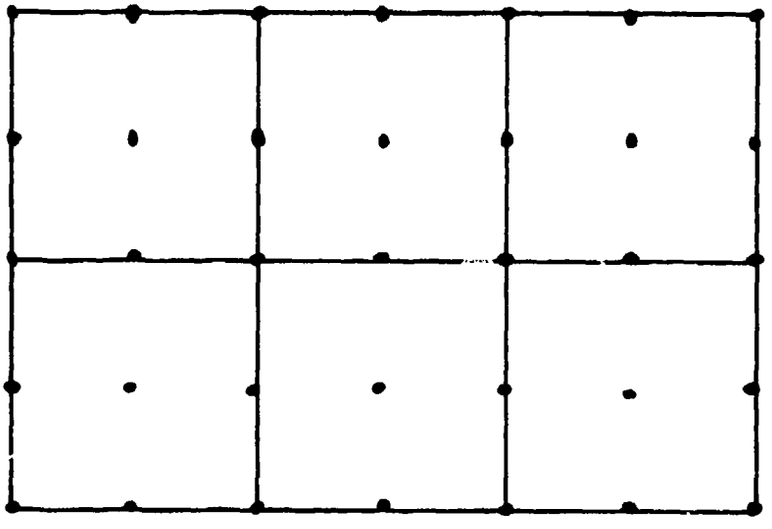

Figure 3b. Location of 35 Nodes on Rectangle with Quadratic Elements

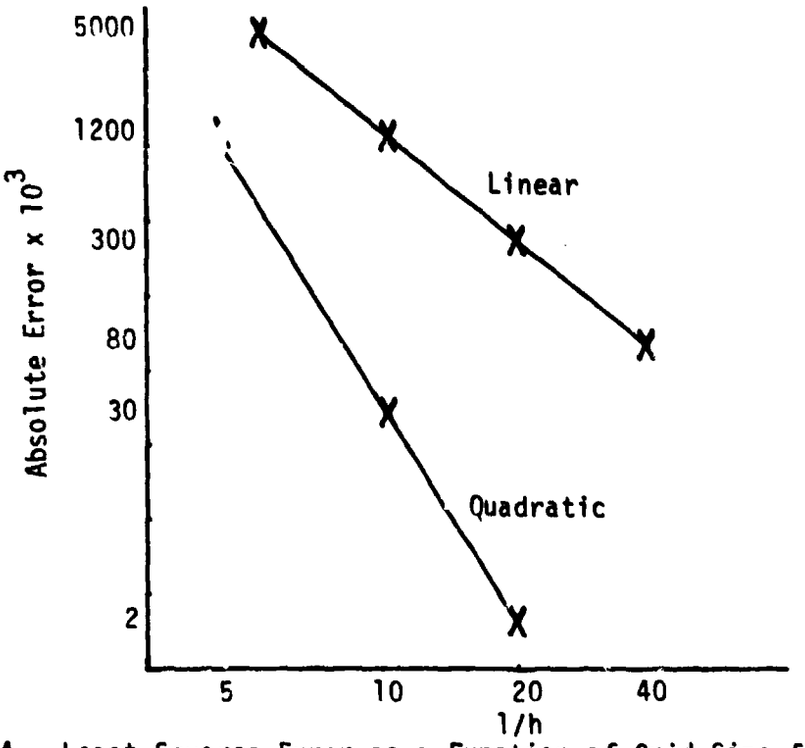

Figure 4. Least Squares Error as a Function of Grid Size for Linear and Quadratic Basis Functions

that is, $p_2 = \frac{\partial p_1}{\partial x}$, $p_3 = \frac{\partial p_1}{\partial y}$, $\frac{\partial p_2}{\partial x} + \frac{\partial p_3}{\partial y} + a^2 p_1 = 0$, with $p_1 = 1$ for $x = 0$, $p_3 = 0$ for $v = 0$ and for $y = 1$, and $p_2 + i\, a\, p_1 = 0$ for $x = 1$. The solutions obtained by using the bilinear basis functions and the biquadratic basis functions were compared to the exact solution for several different grids, and the error is plotted as a function of grid size in Figure 4. The error for bilinear basis functions varies as the second power of the mesh size, while the error for the biquadratic basis functions varies as the fourth power of the mesh size. Therefore, reducing the mesh size by a factor of two reduces the error by a factor of four if bilinear basis functions are used while it reduces the error by a factor of sixteen when biquadratic basis functions are used. As a result of this experience, it was decided to use the biquadratics and obtain the improved accuracy with less computational time.

One final decision that was made was how to handle the nonuniform geometries. The most straightforward approach was to use rectangles and triangles with the triangles used to approximate the boundary as indicated in Figure 1. However, as a test, the case of no-flow in a hard-walled uniform duct was considered. With a plane wave as input and an appropriate exit impedance, the exact solution would be $p(z,r) = \cos(az)-i \sin(az)$ where a is the specified frequency. With rectangular elements, the finite element solution duplicated the exact solution, particularly in the respect that the solution was independent of the variable r; that is, there was no variation in the r direction. When triangular elements were specified by dividing each rectangle into two triangles as indicated in Figure 5, the error increased, and the finite element solution varied incorrectly as a function of r. This is consistent with the observations of Reference 4. With this experience, it was decided to look closely at the isoparametric transformations and the use of quadrilaterals with curved boundaries. In Figure 6, the two ducts which were depicted in Figure 1 are subdivided into curve-sided quadrilaterals. The two main difficulties with using these elements is the definition of the biquadratics on such a nonuniform geometry and the integration over such a geometry. The advantages are the improved approximation of curved boundaries and the ease of generating the elements or subdivisions. The two disadvantages are easily overcome by mapping the nonuniform element to a square as indicated in Figure 7. On the square the mapped biquadratics become the usual biquadratics, and the integration is straightforward. The apparent difficulty of determining the mapping function is also easily resolved. The step which makes the mapping easy is the approximation of the original nonuniform geometry by piecewise quadratics around the boundary and requiring the sides of the quadrilateral elements with curved sides to be quadratic curves. Then the map from the (ξ,η) plane to the (z,r) plane in Figure 7 is the biquadratic which maps each of the nine nodes in the (ξ,η) plane to the appropriate node of the nonuniform element in the (z,r) plane. But any biquadratic on the (ξ,η) square can be written as a linear

combination of the nine elementary biquadratic basis functions defined there. That is, if the map from the (ξ,η) plane to the (z,r) plane is $z = z(\xi,\eta)$ and $r = r(\xi,\eta)$ then z and r can be written as:

$$z=z(\xi,\eta)=\sum_{j=1}^{9} a_j\, g_j(\xi,\eta)$$

$$r=r(\xi,\eta)=\sum_{j=1}^{9} b_j\, g_j(\xi,\eta) \qquad (13)$$

To determine the nine coefficients a_j, $j = 1$ to $j = 9$, and the nine coefficients b_j, $j = 1$ to $j = 9$, one needs to recall that $z_k = z(\xi_k,\eta_k) = \sum_{j=1}^{9} a_j\, g_j\,(\xi_k,\eta_k)$, that $r_k = r(\xi_k,\eta_k) = \sum_{j=1}^{9} b_j g_j(\xi_k,\eta_k)$ and that $g_j(\xi_k,\eta_k) = 1$ if $j=k$, and $g_j(\xi_k,\eta_k) = 0$ if $j\neq k$. Therefore $a_j = z_j$ and $b_j = r_j$, and the map is determined.

A typical integration in the original (z,r) plane is transformed into an integration in the (ξ,η) plane as follows:

$$\iint_{11} f(z,r)\, p(z,r)\, \frac{\partial p}{\partial z}\, dz\, dr$$

$$= \iint_{00} f(z(\xi,\eta),r(\xi,\eta))\, p(z(\xi,\eta),r(\xi,\eta))$$

$$\left(\frac{\partial p}{\partial \xi}\,\frac{\partial \xi}{\partial z} + \frac{\partial p}{\partial \eta}\,\frac{\partial \eta}{\partial z}\right) J(\xi,\eta)\, d\xi\, d\eta \qquad (14)$$

where J is the Jacobian of the transformation and is given by $J = \frac{\partial z}{\partial \xi}\,\frac{\partial r}{\partial \eta} - \frac{\partial z}{\partial \eta}\,\frac{\partial r}{\partial \xi}$. The partial derivatives of ξ and η on the right-hand side of Equation 14 are given by:

$$\frac{\partial \xi}{\partial z} = \frac{\partial r}{\partial \eta}/J,\ \frac{\partial \eta}{\partial z} = \frac{-\partial r}{\partial \xi}/\ J,\ \frac{\partial \xi}{\partial r} = \frac{-\partial z}{\partial \eta}/J,\ \text{and}\ \frac{\partial \eta}{\partial r} = \frac{\partial z}{\partial \xi}\ /J.$$

The actual integration on the right-hand side of Equation 14 is performed with three-point Gaussian quadrature in each of the coordinate directions for a total of nine quadrature points within the square. The results for uniform and nonuniform ducts with and without flow will now be discussed.

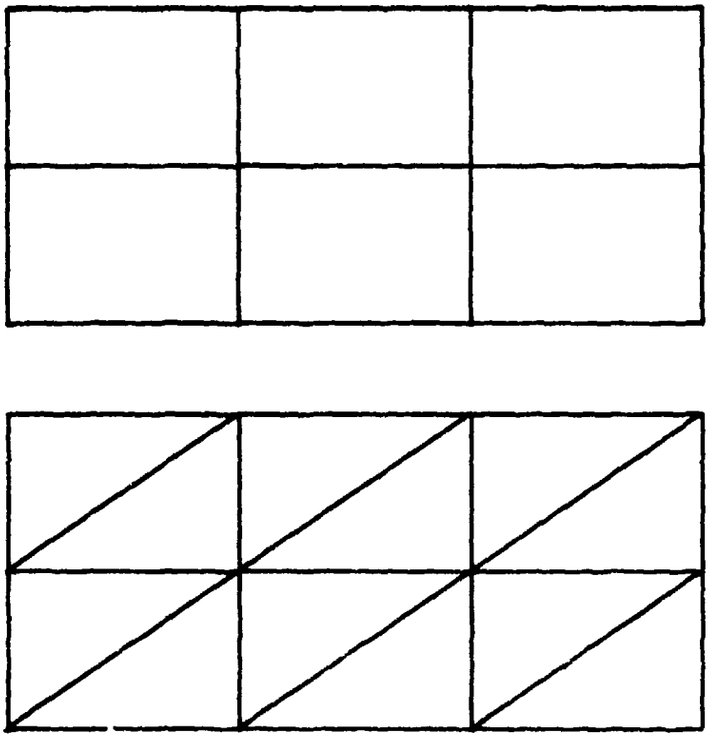

Figure 5. Using 12 Triangular Elements Instead of 6 Rectangular Elements

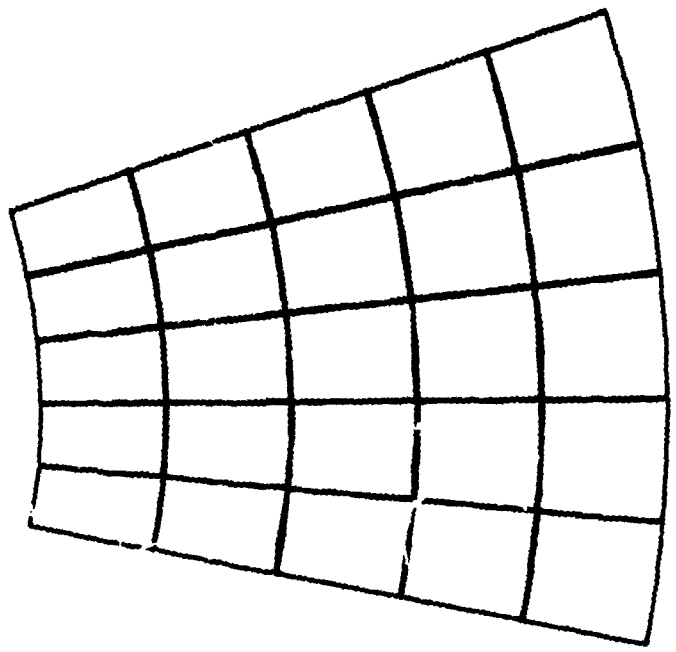

Figure 6a. Quadrilateral Discretization of a Cone

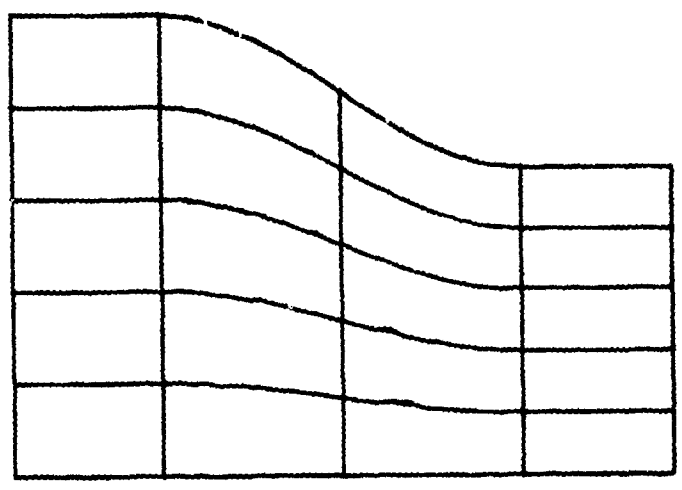

Figure 6b. Quadrilateral Discretization of a Tapered Duct

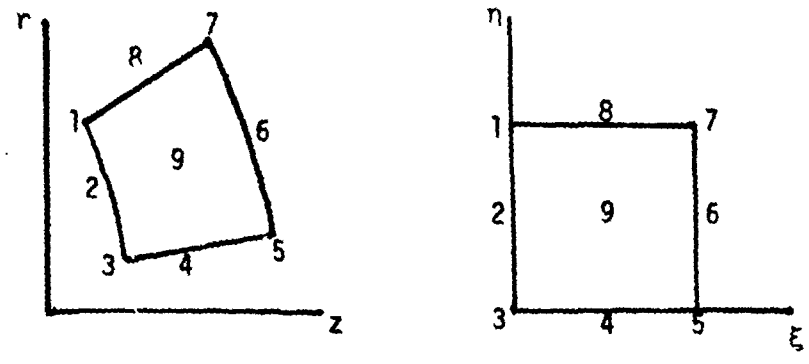

Figure 7. Map of Quadrilateral to a Square

SECTION IV

RESULTS

The first test case for the finite element program was to compute propagation of a plane wave in a hard-walled uniform duct not containing flow. The outstanding agreement with the exact solution is indicated in Figure 8. For a second test case the variation of an individual mode in a soft wall duct not containing flow was computed. As seen in Figure 9, the agreement between the finite element solution and the exact solution is good but not as good as for the plane wave. This is due to the variation in the radial direction. For the cases of uniform flow in a uniform duct, a Mach number of .2 with both a plane wave in a hard wall duct and a single mode in a soft-walled duct was considered. In Figures 10 and 11 the comparisons between the finite element and exact solutions are indicated. Again, the agreement is good, with agreement for the plane wave in the hard wall duct outstanding. For a nonuniform duct the two geometries of Figure 6 were considered to be typical. The cone was most interesting because the exact solution for a plane wave propagating in a hard-walled cone is known and because the finite difference conformal map solution is available. In Figures 12a and 12b the results for a plane wave propagating in a hard-walled cone for two different discretizations are depicted. For the cone, the agreement with exact solution is not as good for the finite element method as for the finite difference method. This is because the finite difference method uses an exact map to a uniform duct while the finite element solution method approximates the circular inlet and exit as piecewise quadratic. This is shown by the decrease in accuracy in Figure 12b where the number of elements in the radial direction was reduced in comparison with the number in Figure 12a.

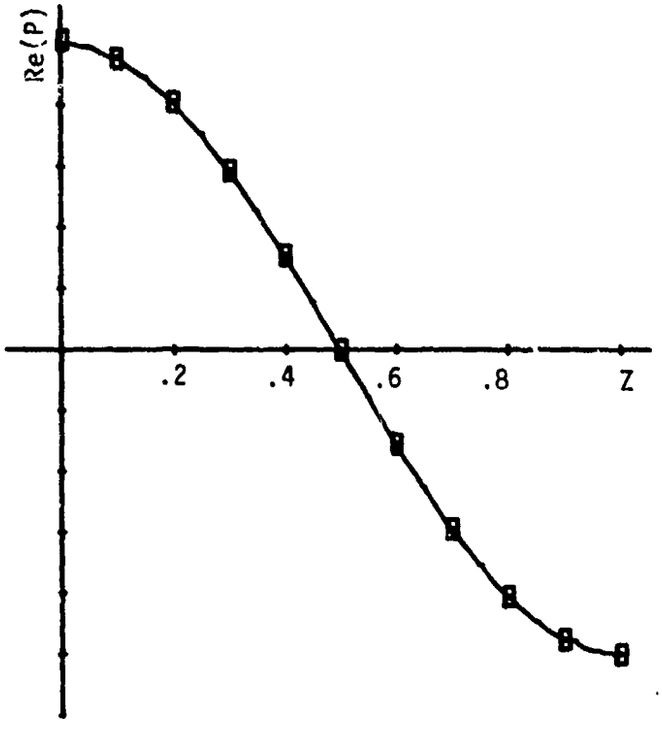

Figure 8. Plane Wave in Hard Wall Cylindrical Duct
M = 0, $\lambda = \pi$

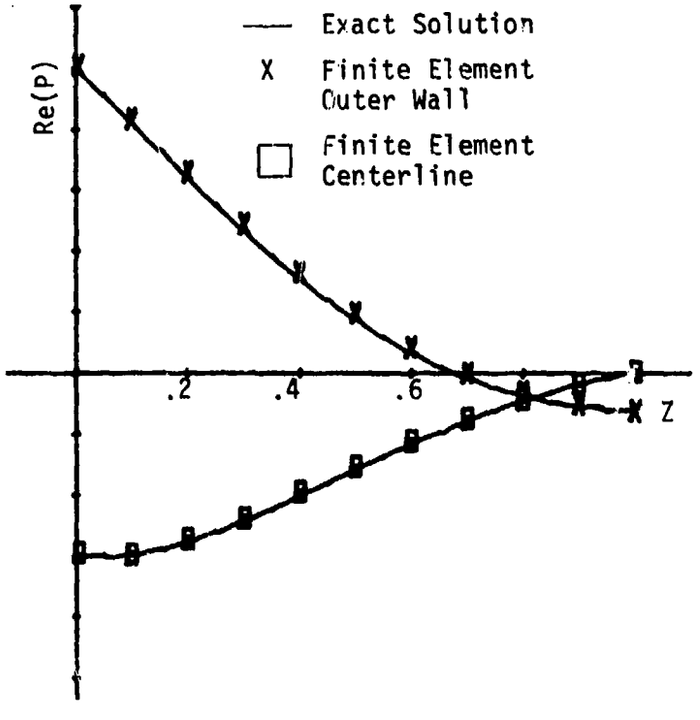

Figure 9. Mode in a Cylindrical Duct;
Mach Number = 0, $\lambda = \pi$

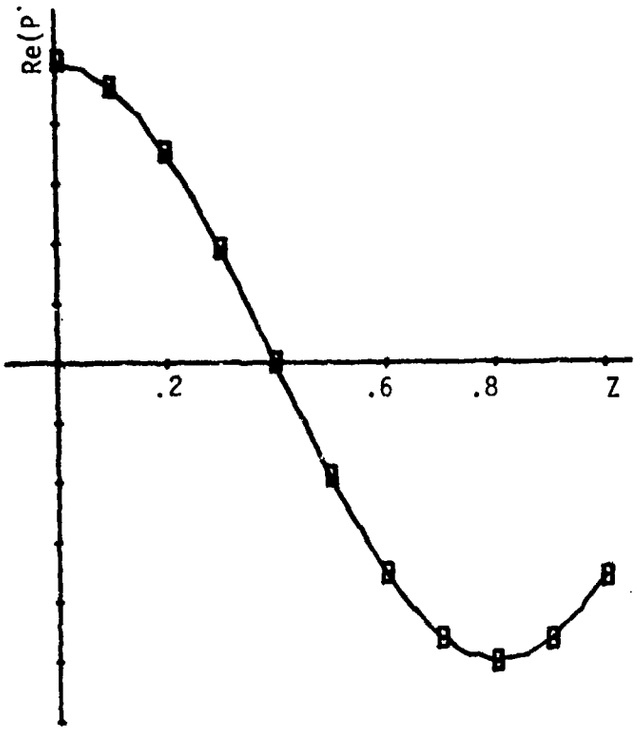

Figure 10. Plane Wave in Hard Wall Cylindrical Duct, M = .2, λ = 4.7

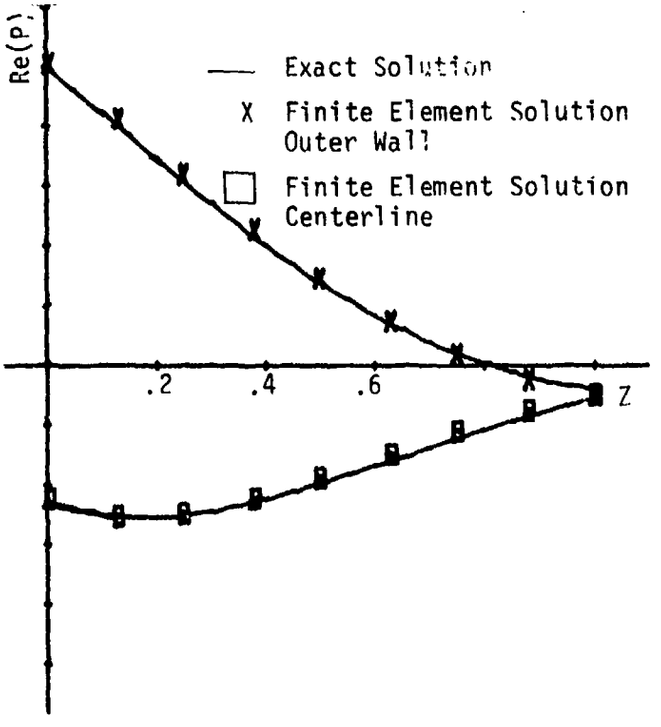

Figure 11. Mode in a Cylindrical Duct; Mach Number = .2, $\lambda = \pi$

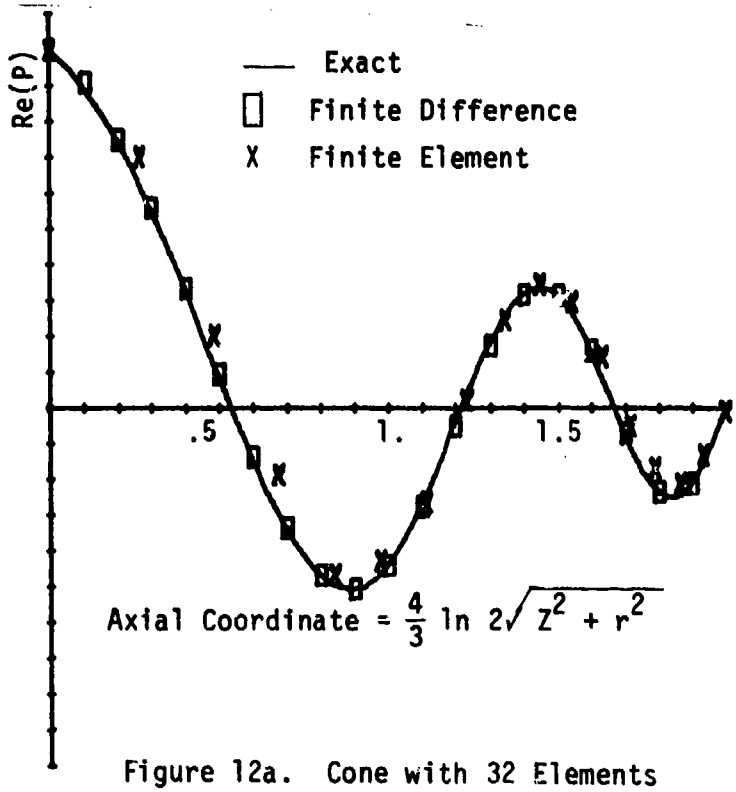

Figure 12a. Cone with 32 Elements
4 in Radial Direction
8 in Axial Direction

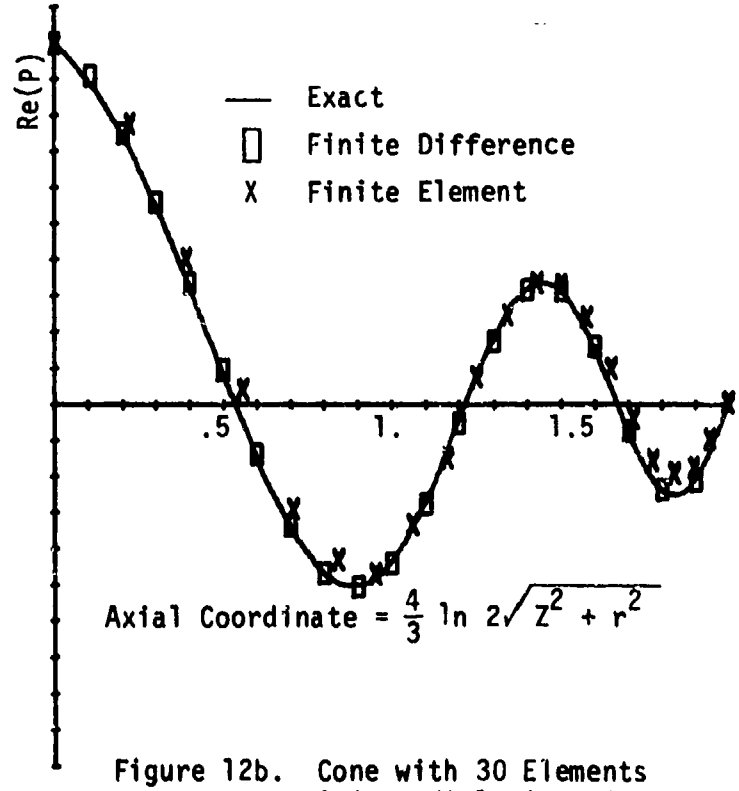

Figure 12b. Cone with 30 Elements
3 in Radial Direction
10 in Axial Direction

REFERENCES

1. Quinn, D.W., "Finite Difference Method for Computing Sound Propagation in Nonuniform Ducts", AIAA Journal, Volume 10, pp. 1392-1394, October 1975.

2. Quinn, D.W., "Attenuation of the Sound Associated with a Plane Wave in a Multisectional Duct", Aeroacoustics: Fan Noise and Control; Duct Acoustics; Rotor Noise, Progress in Astronautics and Aeronautics, Volume 44, The MIT Press, Cambridge, 1976.

3. Quinn, D.W., "Integral Equation Methods in Duct Acoustics for Nonuniform Ducts with Variable Impedance", AIAA Journal, Volume 15. pp. 278-281, February, 1977.

4. Huyakorn, P.S., Taylor, C., Lee, R.L., and Gresho, P.M., "A Comparison of Various Mixed-Interpolation Finite Elements in the Velocity-Pressure Formulation of the Navier-Stokes Equations", Computers and Fluids, Volume 6, pp. 25-35, 1978.

5. Sigman, R.K., Majjigi, R.K., and Zinn, B.T., "Use of Finite Element Techniques in the Determination of the Acoustic Properties of Turbofan Inlets", AIAA paper 77-18, AIAA 15th Aerospace Sciences Meeting, Los Angeles, California, January 24-27, 1977.

6. Eversman, W., Astley, R.J., and Thanh, V.P., "Transmission in Nonuniform Ducts--A Comparative Evaluation of Finite Element and Weighted Residual Computational Schemes", AIAA paper 77-1298, AIAA 4th Aeroacoustics Conference, Atlanta, Georgia, October 3-5, 1977.

7. Abrahamson, A.L., "A Finite Element Algorithm for Sound Propagation in Axisymmetric Ducts Containing Compressible Mean Flow", AIAA paper 77-1301, AIAA 4th Aeroacoustics Conference, Atlanta, Georgia, October 3-5, 1977.

8. Strang, G., Fix, G.J., An Analysis of the Finite Element Method, Prentice-Hall, Englewood Cliffs, New Jersey, 1973.

9. Isaacson, E. and Keller, H.B., Analysis of Numerical Methods, John Wiley & Sons, New York, 1966.